Journal of the Korean Society of Marine Engineering, Vol.30, No.4, pp.463~473, 2006(ISSN 1226-9549)

Study on High Performance and Compact Absorber Using Small Diameter Heat Exchanger Tube

Jung-In Yoon† · Thanh Tong Phan* · Choon-Geun Moon** · Eun-Pil Kim** · Jae-Dol Kim*** and Ki-Cheol Kang****

(Manuscript : Received DEC 9, 2005 ; Revised MAR 24, 2006)

Abstract : The effect of tube diameter on heat and mass transfer characteristics of absorber in absorption chiller/heater using LiBr solution as a working fluid has been investigated by both of numerical and experimental study to develop a high performance and compact absorber. The diameter of the heat exchanger tube inside absorber was changed from 15.88mm to 12.70mm and 9.52mm. In numerical study a model of vapor pressure drop inside tube absorber based on a commercial 20RT absorption chiller/heater was performed. The effect of tube diameter, longitudinal pitch, vapor Reynolds number, longitudinal pitch to diameter ratio on vapor pressure drop across the heat exchanger tube banks inside absorber have been investigated and found that vapor pressure drop decreases as tube diameter increases, longitudinal pitch increases, vapor Reynolds number decreases and longitudinal pitch to diameter ratio increases. In experimental study, a system includes a tube absorber, a generator, solution distribution system and cooling water system was set up. The experimental results shown that the overall heat transfer coefficient, mass transfer coefficient, Nusselt number and Sherwood number increase as solution flow rate increases. In both of study cases, the heat and mass transfer performance increases as tube diameter decreases. Among three different tube diameters, the smallest tube diameter 9.52mm has highest heat and mass transfer performance.

Key words : Tube absorber, Absorption chiller/heater, Lithium bromide aqueous solution, Heat and mass transfer performance, Pressure drop

Nomenclature

A : heat transfer area, m^2
C : concentration, wt%
c_p : specific heat at constant pressure, J/kgK
D : diffusion coefficient, m^2/s
d : tube diameter, m

† Corresponding Author (School of Mechanical Engineering, Pukyong National University, KOREA). E-mail : yoonji@pknu.ac.kr, Tel : 051)620-1506
* Graduate School, Department of Refrigeration and Air-conditioning Engineering, Pukyong National University, KOREA.
** School of Mechanical Engineering, Pukyong National University, KOREA.
*** Department of Environmental Equipment Engineering, Tongmyong University, KOREA.
**** Donghwa Air-conditioning Co., Ltd., KOREA.

h : heat transfer coefficient, W/m^2K
h_{mass} : mass transfer coefficient, m/s
k : thermal conductivity, W/mK
L : tube length, m
M : mass transfer rate, kg/s
Nu : Nusselt number
P : pressure, Pa
Pr : Prandtl number
Re : Reynolds number
Q : heat transfer rate, W
S_L : longitudinal pitch, m
T : temperature, K
U : overall heat transfer coefficient, W/m^2K
u : velocity in x-direction, m/s
v : velocity in y-direction, m/s
x : coordinate in direction of flow, m
y : coordinate in direction perpendicular to flow, m

Greek letters

δ : solution film thickness, m
μ : dynamic viscosity, Pas
v : kinematic viscosity, m^2/s
ρ : density, kg/m^3
Γ : liquid mass flow rate per unit length, kg/ms

Subscripts

c : cooling water
i : inside
in : inlet
o : outside
out : outlet
s : solution
v : vapor

1. Introduction

In recent years, the usage of absorption chiller/heater is positively encouraged for the unused energy application, the preservation of earth environment, and the settlement of unbalanced demand between electric power and natural gas. However, the size of absorption chiller/heater is larger than that of vapour compression type chiller/heater based on the same capacity. An absorption chiller/heater is composed of an absorber, an evaporator, a condenser, a generator, and a solution heat exchanger. Among these components, the absorber has the largest heat transfer area and therefore most expensive component. An optimal design of the absorber is essential for efficient absorption machines. The size of absorber can be reduced by using small diameter heat exchanger tubes to replace conventional diameter heat exchanger tube. Most of previous studies were conducted on tube absorber which made by conventional diameter heat exchanger tube. The tube diameter is usually 19.05mm. The information of tube absorber using small diameter tube has been lacked (Hoffmann et al.[1], Furukawa et al.[2], Yoon et al.[3], Nagaoka et al.[4], Kawamata et al.[5]).

In this paper, the enhancement of the heat and mass transfer in absorber working with LiBr solution by using three different tube diameters 15.88mm, 12.70mm and 9.52mm are tested with both of numerical and experimental study. In numerical study, a model of vapor pressure drop inside tube absorber based on a commercial 20RT absorption chiller/heater was performed. The heat and mass transfer performances has been studied by investigating the effect of tube diameter, longitudinal pitch of tube bank, Reynolds number of water vapor, longitudinal pitch to diameter ratio on the vapor pressure

drop across the heat exchanger tube banks inside absorber.

In experimental study, a system includes a tube absorber, a generator, solution distribution system and cooling water piping system was set up. The effect of tube diameter on overall heat transfer coefficient and mass transfer coefficients, Nusselt number and Sherwood number with different solution flow rates has been investigated.

2. Numerical study

2.1 Model description

In the horizontal tube absorber, the strong LiBr solution film composed of LiBr (absorbent) liquid water (refrigerant) flows down over tube surfaces. The film solution is in contact with water vapor which comes from evaporator. The water vapor is absorbed into solution as water vapor pressure is higher than the partial pressure of liquid water in solution. The amount of the vapor absorbed depends on the value of water vapor pressure. Pressure drop happens as vapor flow across the tube banks and influences to the amount of absorbed vapor. The pressure drop of absorber is different from pressure drop of conventional heat exchanger in calculation as found in several previous studies (Nishimura et al.[6], Wang et al.[7], Wilson et al.[8]), because there is no vapor flow at the outlet absorber.

Table 1 shows the specifications of absorber of 20RT commercial absorption chiller/heater. Based on this reference absorber, a model of vapor pressure drop across the tube banks inside absorber was performed as shown in fig. 1. The tube banks are uniform and staggered, the water vapor flows across tube banks in x direction. Due to symmetry of the tube banks and the periodicity of the flow inherent in the tube banks geometry, only a portion of the geometry is modeled, with symmetry applied to the outer boundary.

Table 1 Specification of absorber of 20RT commercial absorption chiller/heater

Parameters	Values
Tube length [m]	2
Diameter [m]	0.01588
Number of columns of tube bank	13
Number of rows of tube bank	35
Number of tubes in tube bank	228
Longitudinal pitch [m]	0.017
Transverse pitch [m]	0.025620838
Longitudinal pitch to diameter ratio	1.07
Width of absorber [m]	0.238
Height of absorber [m]	0.461175079
Volume of absorber [m^3]	0.219519337
Cooling capacity of evaporator [kW]	70.34
Total vapor mass flow rate [kg/s]	0.028262678
Vapor temperature [°C]	5
Vapor Reynolds number	56
Physical properties of saturated water vapor	
Density [kg/m^3]	0.006802
Dynamic viscosity [kg/ms]	9.34×10^{-6}
Heat of evaporation [kJ/kg]	2488.6904

The inflow boundary is redefined as a periodic zone, and the outflow boundary defined as its shadow. A CFD software, Fluent, is used for the numerical analysis. The studied model shown in fig. 2 is created and meshed by using Gambit software. Quadrilateral cells that provides better resolution of the viscous gradients near the tube walls are used in the regions surrounding the tube walls whereas

triangular cells are used for the rest of domain, resulting in a hybrid mesh with 5792 cells. Then, the created model in Gambit software is exported to the Fluent software in which boundary conditions and material properties are defined.

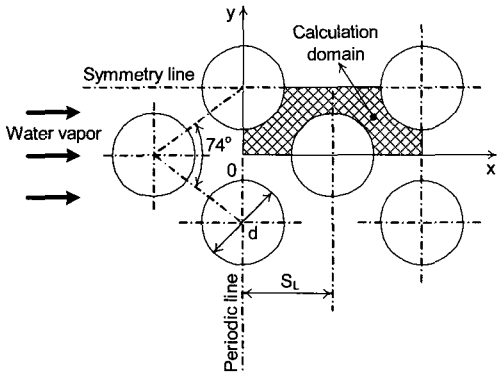

Fig. 1 Schematic of tube banks model inside horizontal tube absorber

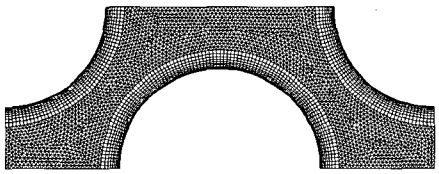

Fig. 2 Grid system of calculation domain

2.2 Governing equations and boundary conditions

In formulating this model, it is assumed that the vapor flow is incompressible, steady and laminar. Neglecting the effect of solution droplets and falling films on vapor pressure drop. Because there is no vapor flow at the outlet absorber, therefore the mass flow rate of absorbed vapor is assumed reduced 50%.

Under the above assumption, the vapor pressure drop across the tube bank inside absorber described by the following equations:

Mass conservation equation is expressed as

$$\frac{\partial u_v}{\partial x}+\frac{\partial v_v}{\partial y}=0 \qquad (1)$$

Momentum equation is expressed by following equations

x-momentum:

$$\rho_v\left(u_v\frac{\partial u_v}{\partial x}+v_v\frac{\partial u_v}{\partial y}\right)=-\frac{\partial p_v}{\partial x}+\mu_v\left(\frac{\partial^2 u_v}{\partial x^2}+\frac{\partial^2 u_v}{\partial y^2}\right) \qquad (2a)$$

y-momentum:

$$\rho_v\left(u_v\frac{\partial v_v}{\partial x}+v_v\frac{\partial v_v}{\partial y}\right)=-\frac{\partial p_v}{\partial y}+\mu_v\left(\frac{\partial^2 v_v}{\partial x^2}+\frac{\partial^2 v_v}{\partial y^2}\right) \qquad (2b)$$

Symmetry boundary and periodic boundary conditions have been applied as mentioned above. The material of tube is assumed to be copper.

2.3 Numerical results and discussions

The volume of absorber is assumed to be constant in order to compare heat and mass transfer performances of three different tube diameters. The software is run for each model to obtain numerical results.

The typical velocity of vapor flow is shown in fig. 3. The typical pressure distribution is shown in fig. 4, as well. The resulting velocity and pressure fields show completely periodic according to the periodic boundary condition.

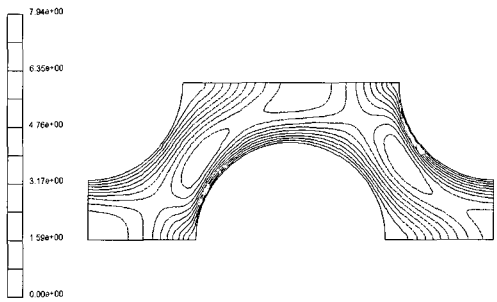

Fig. 3 Velocity distribution of vapor flow

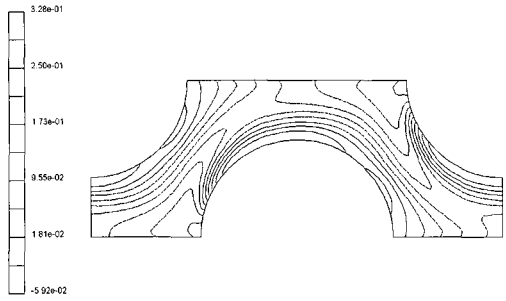

Fig. 4 Pressure distribution of vapor flow

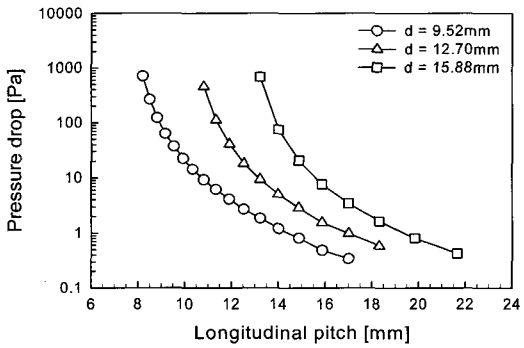

Fig. 5 Effect of longitudinal pitch on pressure drop

Fig. 5 shows the effect of longitudinal pitch on pressure drop. The pressure drop decreases as longitudinal pitch increases. The effect of longitudinal pitch on cooling capacity is shown in fig. 6. The heat and mass transfer performance of three different tube diameters are compared by comparing cooling capacity of three different absorbers which have the same volume and pressure drop of the tube bank but different tube diameter. As shown in fig. 5 and 6, cooling capacity increases as tube diameter decreases. In the case of tube diameter 15.88mm, the longitudinal pitch is 17mm then the pressure drop is 3.448Pa and cooling capacity is 70.34kW. In the case of tube diameter 12.70mm and 9.52mm, the longitudinal pitch is 14.6mm and 12.16mm then cooling capacity is 76.95kW and 83.81kW, respectively. It means that in the case of tube diameter 12.70mm and 9.52mm, the cooling capacity is 9.4% and 19.2% higher than the cooling capacity of tube diameter 15.88mm, respectively.

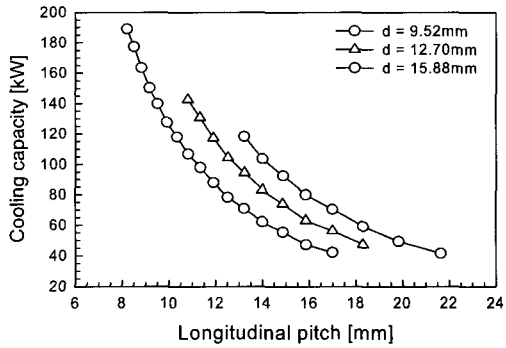

Fig. 6 Effect of longitudinal pitch on cooling capacity

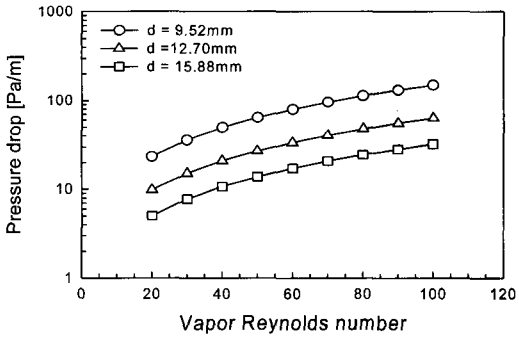

Fig. 7 Effect of vapor Reynolds number on pressure drop

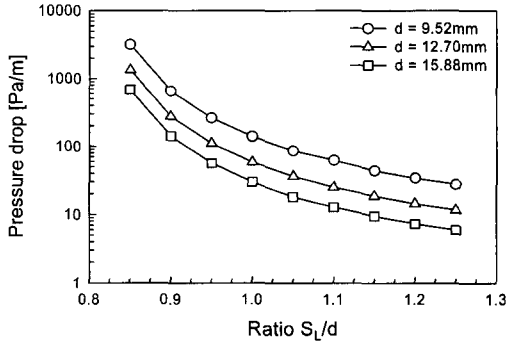

Fig. 8 Effect of longitudinal pitch to diameter ratio S_L/d on pressure drop

The effect of vapor Reynolds number on pressure drop per unit length of the tube bank in flow direction is shown in fig. 7. The pressure drop increases as vapor Reynolds number increases. In the case of small diameter the pressure drop also increases.

Fig. 8 shows the effect of longitudinal pitch to diameter ratio S_L/d on pressure drop per unit length of the tube bank in flow direction. In designing absorber, it is necessary to decrease the longitudinal pitch to diameter ratio S_L/d in order to decrease the absorber size. However as shown in the figure, it makes the pressure drop increases, resulting in working pressure inside absorber increases. That means it exists an optimal longitudinal pitch to diameter ratio S_L/d, it is about 1.0 to 1.1 depending on the tube diameter.

3. Experimental study

3.1 Experimental apparatus

Fig. 9 shows the schematic diagram and photo of experimental apparatus. As shown in the figure, the apparatus consists of an absorber, a generator, solution distribution system and cooling water piping systems. Three different diameter copper tubes are installed in the absorber with the same heat transfer area to compare their heat and mass transfer performances as shows in table 2.

Table 2 Specification of the test tubes

Column number	Number of tubes	Outside diameter (mm)	Inside diameter (mm)	Length (mm)
1	10	15.88	13.84	400
2	12	12.70	10.92	
3	16	9.52	8.00	

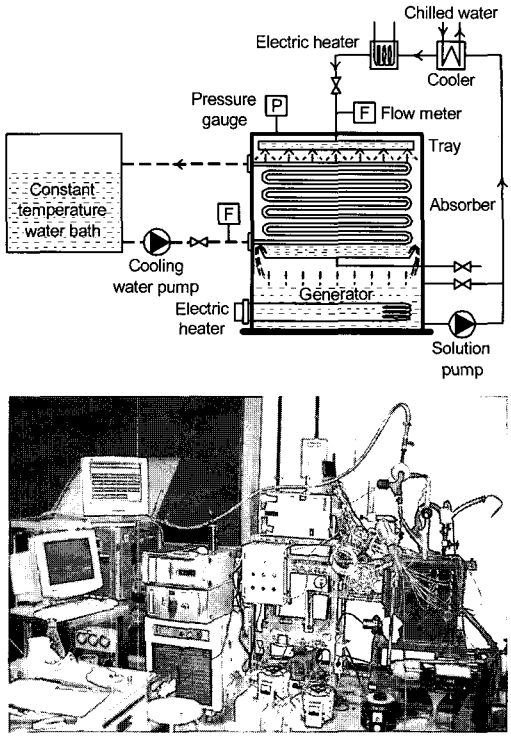

Fig. 9 Schematic diagram and photo of experimental apparatus

A vacuum pump is installed to keep the vacuum pressure constant in the apparatus and a pressure gauge is used to measure the pressure inside absorber. Solution in generator is heated by an electric heater and a circulation solution pump is installed to circulate solution in the absorber and generator. At the inlet absorber, a cooler cooled by chilled water and an electric heater are installed to control the inlet solution temperature. In cooling water piping system, a cooling water pump is used to circulate cooling water in the absorber. A constant temperature water bath is used to contain cooling water as well as control cooling water temperature. The thermocouples are installed to measure the temperature variations of solution and cooling water. The flow meters are installed to measure the flow rates of cooling water and solution regulated by needle

valves. The solution concentration is measure by hydrometer. Finally, a data logger and a computer are used to record the temperature data.

3.2 Experimental method

Experimental conditions are shown in table 3. The experiment was conducted in two processes: the generation process and the absorption process. In the generation process, the water vapor obtained by heating solution in the generator. When the concentration of solution inside generator reaches the experimental condition, heating is stopped and the strong solution is controlled to an assigned temperature by cooler and heater before coming to the absorber.

Table 3 Experimental conditions

Parameters		Conditions
Pressure of absorber [mmHg]		7
LiBr solution	Inlet temperature [°C]	47
	Inlet concentration [wt%]	61
	Flow rate [kg/ms]	0.014-0.032
Cooling water	Inlet temperature [°C]	32
	Flow rate [L/min]	10

In the absorption process, the pressure inside absorber is reduced to 7mmHg by the vacuum pump. The strong solution in the generator is discharged to the top of absorber and flows down outside tube surface through the tray installed at the upper part of absorber. The strong solution absorbs water vapor evaporated from generator and falls back to generator. The other tray is installed at absorber outlet to get the sample of outlet solution. During absorption process, the absorption heat is generated and transported to the tube wall cooled by cooling water maintained inlet temperature at 32°C. Cooling water is circulated counter to solution flow from the bottom to the top of absorber. For the present experiments, the steady state measuring time was approximately 5 minutes for each parameter.

3.3 Calculation method of heat and mass transfer

The logarithmic mean temperature difference for tube bank inside absorber is defined as

$$\triangle T_{lm}=\frac{(T_{s,in}-T_{c,out})-(T_{s,out}-T_{c,in})}{\ln\left[\frac{(T_{s,in}-T_{c,out})}{(T_{s,out}-T_{c,in})}\right]} \quad (3)$$

The heat transfer rate transferred from tube wall to cooling water is

$$Q=M_c c_{p,c}(T_{c,out}-T_{c,in})=UA_o \triangle T_{lm} \quad (4)$$

Where heat transfer area of outside tube surface is $A_o=\pi d_o L$.

An experimental correlation of the convection heat transfer coefficient of the cooling water flowing inside tube given by Dittus-Boelter is

$$Nu_c=0.023 Re_c^{0.8} \Pr_c^{0.4}=\frac{h_i d_i}{k_c} \quad (5)$$

The heat transfer coefficient of liquid film solution flowing outside the tube can be obtained from eq. (6). The thermal resistance of the tube wall is assumed to be negligible.

$$h_o=\left(\frac{1}{U}-\frac{d_o}{d_i h_i}\right)^{-1} \quad (6)$$

The mass flow rate of the solution per unit tube length is expressed as

$$\Gamma_s = \frac{M_s}{2L} \tag{7}$$

The solution film thickness is determined by Nusselt's analysis [7] as follows:

$$\delta = \left(\frac{3\Gamma_s \mu_s}{\rho_s^2 g} \right)^{1/3} \tag{8}$$

And solution film Reynolds number is

$$Re_s = \frac{4\Gamma_s}{\mu_s} \tag{9}$$

The mass flow rate of vapor absorbed in absorption process is given by mass conservation of aqueous solution

$$M_v = M_s \left(\frac{C_{s,in}}{C_{s,out}} - 1 \right) \tag{10}$$

The vapor-liquid interface of liquid falling film is regarded as in thermodynamic equilibrium with the absorber pressure. The logarithmic mean concentration difference is defined as follows

$$\Delta C_{lm} = \frac{(C^*_{s,in} - C_{s,in}) - (C^*_{s,out} - C_{s,out})}{\ln\left[\frac{(C^*_{s,in} - C_{s,in})}{(C^*_{s,out} - C_{s,out})} \right]} \tag{11}$$

Where $C^*_{s,in}$ and $C^*_{s,out}$ are the equilibrium concentration of vapor-liquid interface at the absorber inlet and outlet respectively.

The mass transfer coefficient in the absorption process is

$$h_{mass} = \frac{M_v}{\rho_s A_o \Delta C_{lm}} \tag{12}$$

3.4 Experimental results and discussions

Fig. 10 shows the effect of solution flow rate on overall heat transfer coefficient. The overall heat transfer coefficient increases as solution flow rate increases. At the normal experimental condition, the solution flow rate is 0.025kg/ms, the overall heat transfer of the tube diameter 15.88mm is 0.669W/m^{2}K. In the case of tube diameter 12.70mm and 9.52mm, the overall heat transfer coefficient is 4.2% and 5.7% higher than the overall heat transfer coefficient of tube diameter 15.88mm, respectively. In comparing with previous studies, the overall heat transfer coefficient of this study agrees well with study of Furukawa et al.[2] in all range of solution flow rate and agrees well with study of Yoon et al.[3] at solution flow rate is from 0.01kg/ms to 0.02kg/ms but shows higher value than study of Hoffman et al.[1].

$$Nu_s = \frac{h_o \delta}{k_s} \tag{13}$$

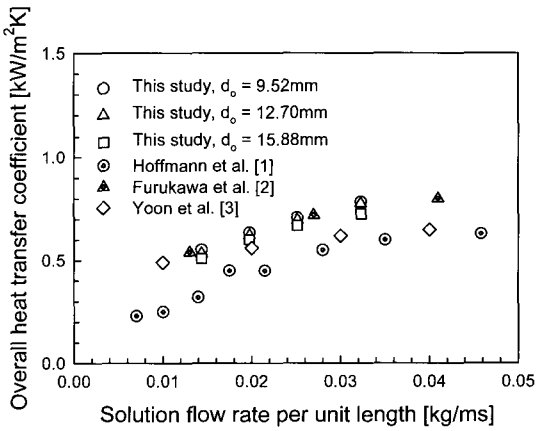

Fig. 10 Effect of solution flow rate on overall heat transfer coefficient

The effect of solution flow rate on Nusselt number is shown on fig. 11. The Nusselt number of solution film is determined by following equation

As shown in the figure, the Nusselt increases as solution flow rate increases. At the normal experimental condition, the Nusselt number the tube diameter 15.88mm is 0.422. In the case of tube diameter 12.70mm and 9.52mm, the Nusselt number is 7.6% and 9.7% higher than the Nusselt number of tube diameter 15.88mm, respectively.

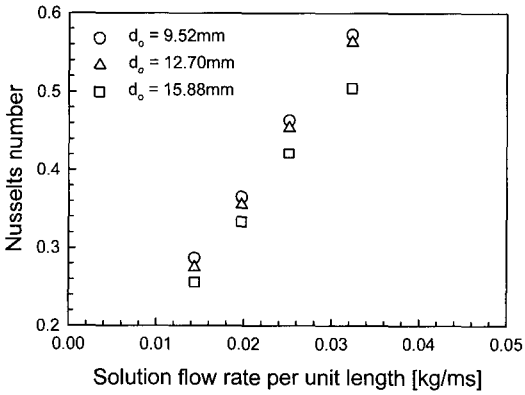

Fig. 11 Effect of solution flow rate on Nusselt number

Fig. 12 shows the effect of solution on mass transfer coefficient. The amount of vapor absorbed into solution increase as the solution flow rate increases, thus the mass transfer coefficient increases. As shown in the figure, the mass transfer coefficient increases as the tube diameter decreases. In the case of tube diameter 12.70mm and 9.52mm, the mass transfer coefficient is 13.6% and 37.7% higher than the mass transfer coefficient of tube diameter 15.88mm, respectively. In comparing with previous studies, the mass transfer coefficient of this study agrees well with studies of Furukawa et al.[2], Nagaoka et al.[4] and Kawamata et al.[5].

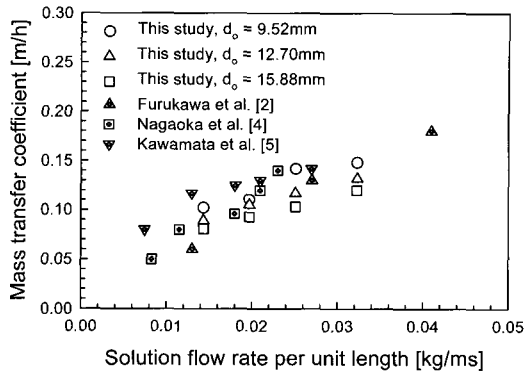

Fig. 12 Effect of solution flow rate on mass transfer coefficient

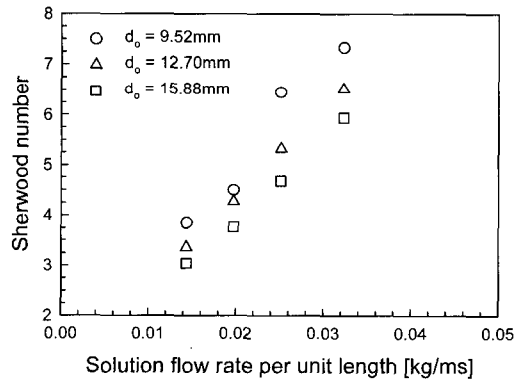

Fig. 13 Effect of solution flow rate on Sherwood number

The effect of solution flow rate on Sherwood number is shown on fig. 13. The Sherwood number of liquid film solution is determined as follows

$$Sh_s = \frac{h_{mass}\delta}{D_s} \tag{14}$$

The mass transfer coefficient increases as the solution flow rate increases and tube diameter decreases hence the Sherwood number also increases.

4. Conclusions

The enhancement of the heat and mass transfer by using three different tube diameters 15.88mm, 12.70mm and 9.52mm are tested with both of numerical and experimental study. The results can be summarized as follows:

In numerical study, vapor pressure drop decreases as tube diameter increases, longitudinal pitch increases, vapor Reynolds number decreases and longitudinal pitch to diameter ratio increases.

In experimental study, the overall heat transfer coefficient, mass transfer coefficient, Nusselt number and Sherwood number increase as solution flow rate increases.

In both of study cases, the heat and mass transfer performance increases as tube diameter decreases. Among three different tube diameters, the smallest tube diameter 9.52mm has highest heat and mass transfer performance.

References

[1] L. Hoffmann, I. Greiter, A. Wagner, V. Weiss and G. Alefeld, "Experimental investigation of heat transfer in a horizontal tube falling film absorber with aqueous solutions of LiBr with and without surfactants", International Journal of Refrigeration, Vol. 19, No. 5, pp. 331-341, 1996.

[2] M. Furukawa, N. Sasaki, T. Kaneko, T. Nosetani, "Enhanced heat transfer tubes for absorber of absorption chiller /heater", Transactions of the JAR, Vol. 10, No. 2, pp. 219-226, 1993.

[3] J. I. Yoon, O. K. Kwon, P. K. Bansal, C. K. Moon, H. S. Lee, "Heat and mass transfer characteristics of a small helical absorber ", Applied Thermal Engineering, Vol. 26, pp. 186-192, 2006.

[4] Y. Nagaoka, N. Nishiyama, K. Ajisaka, O. Kawamata, T. Tadaki, "Study on heat transfer tubes for an absorber of the absorption refrigerator", Proceedings of the 24th National Heat Transfer Symposium of Japan, 2nd Report, pp. 507-509, 1987.

[5] O. Kawamata, T. Otani, N. Oshitulia, T. Aliyanchi, "Development of high performance heat transfer tubes for absorber of absorption refrigerator", Hitachi, No. 8, pp. 57-62, 1989.

[6] T. Nishimura, Y. Kawamura, "Analysis of flow across tube banks in low Reynolds number region", Journal of Chemical Engineering of Japan, Vol. 14, pp. 267-272, 1981.

[7] Y. O. Wang, L. A. Penner, S. J. Ormiston, "Analysis of laminar forced convection of air for crossflow in banks of staggered tubes", Numerical Heat Transfer, Part A, Vol. 38, pp. 819-845, 2000.

[8] A. S. Wilson, M. K. Bassiouny, "Modeling of heat transfer for flow across tube banks", Chemical Engineering and Processing, Vol. 39, pp. 1-14, 2000.

Author Profile

Jung-In Yoon
Birth: 1961. 1988: B.Eng., Pukyong Natl Univ. (PKNU), KOREA. 1995: Ph.D.Eng., Tokyo Univ. of A&T, JAPAN. Current: Associate Prof., PKNU, Shool of Mechanical Engg.

Thanh-Tong Phan

Birth: 1973, 1996: B.Eng., Hochiminh City Univ. of Technology (HUT), VIETNAM. 2000: Lecturer, HUT. 2002: M.Eng., Pukyong Natl Univ. (PKNU), KOREA. Current: Ph.D. Student, PKNU, Dept. of Refrigeration & Air-conditioning Engg.

Choon-Geun Moon

Birth: 1971, 1997: B.Eng., Pukyong Natl Univ. (PKNU), KOREA. 1999: M.Eng., PKNU. 2004: Ph.D.Eng., PKNU, Current: Postdoctoral researcher, Univ. of Auckland, NEW ZEALAND.

Eun-Pil Kim

Birth: 1962. 1987: B.Eng., Pusan Natl Univ., KOREA. 1991: M.Eng., Univ. of Pittsburgh, USA. 1995: Ph.D.Eng., Univ. of Pittsburgh, USA. Current: Assistant Prof., Pukyong Natl Univ., KOREA, Shool of Mechanical Engg.

Jae-Dol Kim

Birth: 1967. 1991: B.Eng., Pukyong Natl Univ. (PKNU), KOREA. 1993: M.Eng., PKNU. 1996: Ph.D.Eng., PKNU. Current: Assistant Prof., Dongmyong Univ., KOREA, Dept. of Environment & Equipment Engg.

Ki-Cheol Kang

Birth: 1965. 1991: B.Eng., Pukyong Natl Univ., KOREA. Current: Director, Dong-hwa Air-conditioning Co., Ltd., KOREA.